BMC Medicine

RESEARCH

Open Access

Integrated serum proteomic and liver genomic analyses identify molecular signatures associated with metabolic dysfunction-associated steatotic liver disease: a multi-cohort study

Jinjian Xu[1,2†], Wanglong Gou[3,4†], Xinyue Wang[2†], Dongmei Ru[2], Wei Hu[2], Jieteng Chen[3,4], Bang-yan Li[2], Yue Xi[2], Ju-Sheng Zheng[3,4*] and Yu-ming Chen[2*]

Abstract

Background Circulating proteomics acts as an intermediate phenotype linking genetic susceptibility to MASLD. However, current evidence rarely establishes a direct concordance between serum protein levels and hepatic gene expression. We aimed to perform a multi-cohort joint analysis of serum proteomics and transcriptomics to characterize essential molecular features for MASLD.

Methods For the serum proteomic analysis of simple steatosis (MASL), we conducted a cross-sectional investigation in an MRI-based cohort (*N*/cases: 1048/428) and further examined the prospective association between protein features and MASL incidence (*N*/cases: 2945/1947) ascertained by ultrasonography over a median 9.8-year follow-up in the Guangzhou Nutrition and Health Study (GNHS) cohort. In parallel, we characterized fibrosis and MASH-related transcriptional features using liver transcriptomics from the MASH cohort ($N=94$) and validated these gene signatures for MASH in liver transcriptomes from the independent Japanese and German populations ($N=98$ and 59).

Results The serum proteomic analysis identified the C3, C9, F9, VTN, AFM, APOD, APOF, and SHBG proteins were significantly associated with MASL risk ($P<0.05$). Liver transcriptomic analysis revealed a coordinated downregulation of C9, C4BPB, C1RL, APOF, and ITIH4 in the high NAS group, implicating dysregulated complement activation as a critical mechanism driving disease progression. Furthermore, SHBG, A2M, GSN, C7, LUM, IGHG3, and IGFALS were associated with liver fibrosis stages, and pathways related to extracellular exosomes and vesicles were implicated in fibrotic development. Consistently, in the Japanese and Germany cohorts, APOF, GSN, and LUM exhibited aberrant expression in both MASH patients and those with high NAS scores.

Conclusions The multi-cohort study identified specific serum protein signatures associated with MASL risk, which correspond to dysregulated gene expression patterns in hepatocytes. These findings bridge the gap

†Jinjian Xu, Wanglong Gou and Xinyue Wang contributed equally as co-first authors.

*Correspondence:
Ju-Sheng Zheng
zhengjusheng@westlake.edu.cn
Yu-ming Chen
chenyum@mail.sysu.edu.cn
Full list of author information is available at the end of the article

between systemic circulatory changes and intrahepatic pathological progression, providing not only robust non-invasive biomarkers for early stratification but also potential mechanistically-driven therapeutic targets for halting the progression of MASLD.

Highlights

- This study identified consistent dysregulation patterns across serum proteomic and liver transcriptomic signatures, spanning MASLD disease stages and multi-ethnic cohorts, establishing an indirect molecular correlation between circulating proteins and hepatic gene expression.
- Liver transcriptomic analysis demonstrated that the downregulation of complement inhibitors (C9, C4BPB, C1RL) and a lipid transport regulator (APOF) may serve as important molecular markers for the progression of MASH.
- Fibrosis-associated molecular signatures, including elevated A2M, GSN, and LUM, are consistently validated across Asian and European cohorts, supporting their broad relevance as biomarkers and therapeutic targets.

Keywords MASLD, Serum proteomics, Liver transcriptomics, Multi-cohort study

Graphical Abstract

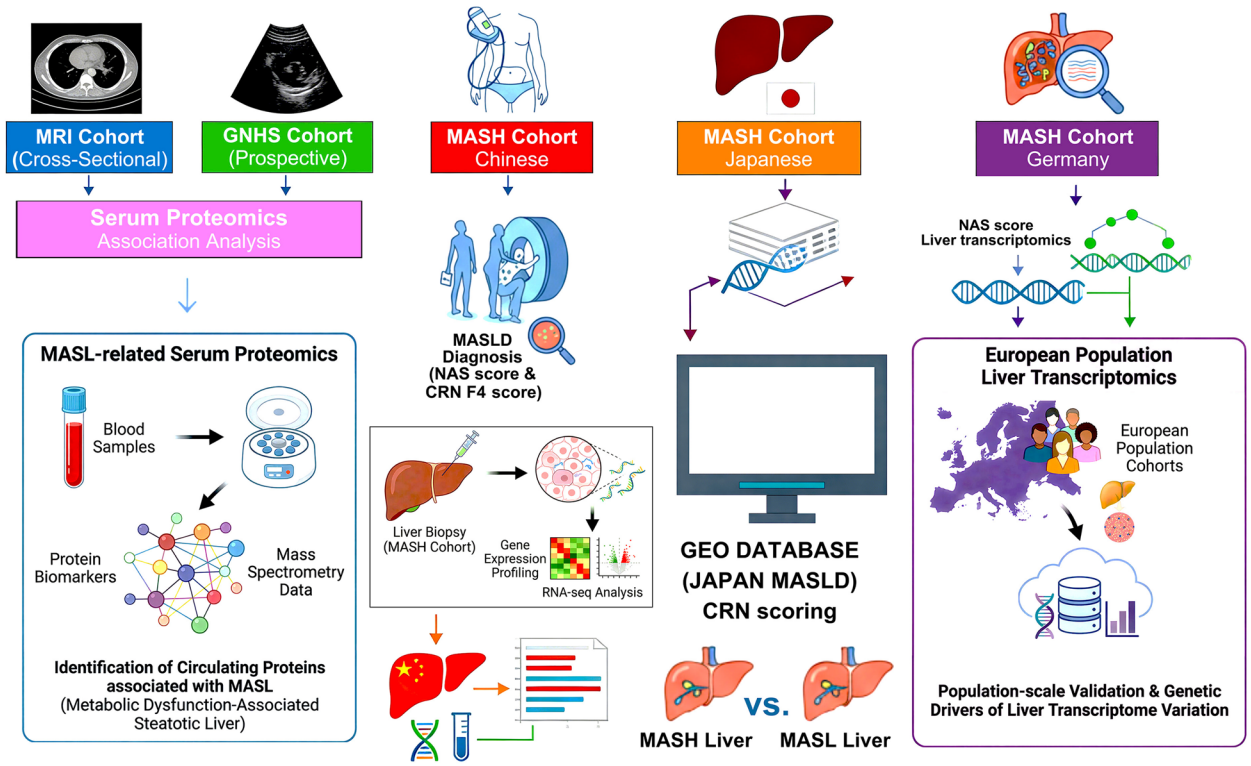

Background

Metabolic dysfunction-associated steatotic liver disease (MASLD) has become the most common chronic liver disease globally, impacting 25–30% of the worldwide population [1]. Approximately one-quarter of individuals with MASLD will progress to metabolic dysfunction-associated steatohepatitis (MASH), which dramatically increases the risk of cirrhosis, hepatocellular carcinoma (HCC), and cardiovascular disease [2, 3]. Although research into the pathogenic mechanisms and therapeutic targets of MASLD has

drawn sustained scientific interest, significant limitations remain in the identification of clinically relevant biomarkers for the disease [4].

Circulating proteomics has emerged as a systematic and high-throughput methodology demonstrating considerable promise for biomarker discovery and the development of diagnostic and predictive models in metabolic disorders, including MASLD [5, 6]. Previous population cohorts have identified numerous plasma protein markers linked to insulin resistance, dyslipidemia, and aging, with the goal of discovering sensitive biomarkers and developing accurate predictive models for metabolic disease progression [7, 8]. Earlier studies have identified multiple circulating proteomic markers for MASLD, advancing the development of non-invasive diagnostic tools for the disease [9, 10]. A 37-protein classifier exhibited excellent predictive capacity, demonstrating training-validation AUC values of 0.95–0.79 for steatosis and 0.92–0.85 for fibrosis staging [11]. Notably, multiple studies confirmed that various plasma proteins were significantly associated with the risk of MASLD [12], including key molecules such as complement proteins (C3, C7, and C9), inflammation-related proteins (RBP4, CD14, IGFBP2, and IGFBP7), and apolipoproteins (APOE, APOD, and APOA) [13]. Several of these proteins have been validated in relation to hepatic fat content and disease severity, offering valuable insights into the systemic pathophysiology of MASLD [10]. However, plasma proteomic signatures reflect a systemic, multi-organ integrated signal, hindering precise identification of liver-specific pathological processes and accurate characterization of intrahepatic intercellular crosstalk and microenvironmental changes [9]. Liver biopsy remains the diagnostic gold standard and continues to be indispensable for accurate histopathological grading and assessment of disease progression [14]. In MASLD biomarker research, single-omics analyses often fail to comprehensively elucidate the pathological relationships between molecular signatures and disease phenotype [10]. Therefore, an integrated multi-omics approach combining circulating proteomics with liver transcriptomics may offer a more effective strategy for uncovering core molecular drivers of disease progression [15].

This study established an integrated research framework combining cross-sectional and prospective designs to characterize the molecular landscape of MASLD. Serum proteomic profiling was performed using liquid chromatography-tandem mass spectrometry (LC–MS/MS) to identify circulating protein signatures. We first employed a cross-sectional cohort, in which MASL was diagnosed non-invasively using MRI. This prospective cohort study employed abdominal ultrasonography for MASL diagnosis, enabling the establishment of the temporal relationship between serum proteomic signatures and MASL progression. Concurrently, transcriptomic profiling was conducted on liver biopsy specimens from a Chinese MASH cohort to investigate differential gene expression associated with NAFLD Activity Score (NAS) and fibrosis stage. We further validated these findings in Japanese and German cohorts via liver transcriptomic profiling, with a focus on gene expression patterns associated with NAS score and MASH.

Methods

Study population

The participants of serum proteomic study for MASL were from the Guangzhou Nutrition and Health Study (GNHS; NCT03179657), a 2008-initiated cohort comprising 4048 baseline participants aged 40–75 years [16]. A total of 3415 participants were enrolled at baseline and underwent three follow-up surveys over a median follow-up period of 9.8 years. The MRI study population was drawn from the GNHS cohort and consisted of participants enrolled in a supplementary survey conducted between 2020 and 2023 ($n=1180$). All participants were confirmed free of viral hepatitis, chronic hepatic disorders (including hepatitis and cirrhosis), and MASLD-targeting medications for at least 12 months prior to enrollment (Additional file 1: Fig. S1A and B). In the Zhejiang MASH cohort ($n=94$), middle-aged and older participants underwent histopathological adjudication via liver biopsy following initial MRI-based diagnosis, providing a basis for integrated liver transcriptomic profiling.

The study protocol was approved by the Institutional Review Board of Sun Yat-sen University's School of Public Health and Zhejiang Provincial People's Hospital (Affiliated People's Hospital, Hangzhou Medical College), and written informed consent was obtained from all participants.

Collection of covariates

Following 12-h overnight fasting, venous blood was drawn into EDTA and non-EDTA vacutainers from all subjects. EDTA tubes underwent 1500 × g centrifugation (15 min, 4 °C) within 2 h for plasma isolation, while serum was obtained from non-EDTA tubes centrifuged at 1811 g for 10 min. All aliquots were vortexed and stored at − 80 °C until analysis. Trained personnel obtained anthropometric data and administered structured interviews capturing medical history, sociodemographics, lifestyle factors, and dietary patterns using a validated quantitative food frequency questionnaire (FFQ). Specific items assessed hepatitis status, hepatotoxic medication use, and alcohol consumption. Anthropometric measurements were measured by trained staff. In biochemistry, all samples were analyzed in a single

batch within 5 days to minimize laboratory variability. Plasma total cholesterol (TC), triglycerides (TG), HDL cholesterol (HDL-C) and LDL cholesterol (LDL-C), fasting plasma glucose (FPG), and uric acid (UA) were measured. The methods and contents of biochemical indexes were presented in Additional file 1: Method 1.

Abdominal radiomics and definition of MASLD

Hepatic steatosis (HS) severity and degree were non-invasively evaluated using MRI and ultrasonography [17, 18]. MRI proton density fat fraction (MRI-PDFF) demonstrates high diagnostic sensitivity, capable of detecting hepatic steatosis at thresholds as low as 5% [19]. Doppler ultrasonography (Sonoscape SSI-5500, China) was conducted by blinded radiologists [17]. Hepatic steatosis was defined by the presence of at least two of three abnormal findings on abdominal ultrasonography: diffusely increased echogenicity ("bright") liver with liver echogenicity greater than the kidney or spleen, vascular blurring, or deep attenuation [20]. The NASH Clinical Research Network (NASH-CRN) Pathology Committee's scoring system classified hepatic steatosis severity into grades 0–3 (absent, mild, moderate, severe) based on hepatocellular fat content (< 5%, 5–33%, 33–66%, > 66%) [21]. Diagnosis of MASLD was established according to the international expert consensus statement [22], with the requirement of at least one comorbid cardiometabolic abnormality. Detailed diagnostic criteria and workflow are provided in Additional file 1: Method 2 and Additional file 1: Fig. S2, respectively.

Serum proteomics profiling and preprocessing

Serum proteomic profiling was performed using LC–MS/MS in the MRI cohort and the Guangzhou Nutrition and Health Study (GNHS) cohort, enabling the quantification of 326 proteins. The GNHS cohort included three longitudinal follow-up waves: wave 1 ($n = 3415$), wave 2 ($n = 2567$), and wave 3 ($n = 1722$). In the GNHS cohort, baseline serum proteomic profiles had been used as exposure data, with a mean follow-up of 9.8 years from the time of proteomic measurement to the occurrence of the primary outcome events. In the MRI cohort, serum proteomic measurements and outcome assessments had been conducted concurrently at the same time point. A targeted serum proteomic analysis was performed using liquid chromatography-tandem mass spectrometry (LC–MS/MS) with selective/multiple reaction monitoring (SRM/MRM) [23]. Proteins were enzymatically digested into peptides, followed by desalting and chromatographic separation using a C18 column with a 30-min gradient. Mass spectrometric detection was conducted in positive ion mode with predetermined precursor-product ion transitions for quantitative analysis. Further details on LC–MS/MS methodology are available in Additional file 1: Methods 3 and 4.

Transcriptomic mRNA sequencing of human liver tissue

Based on the Zhejiang MASH cohort, we performed liver biopsies in 94 patients with MRI-confirmed MASLD to evaluate the NAFLD Activity Score (NAS) and assess the degree of liver fibrosis using the NAS-CRN scoring system. Eligible participants met the following criteria: (1) imaging-confirmed hepatic steatosis; (2) persistent elevation of liver enzymes; (3) absence of other chronic liver diseases, including viral and autoimmune hepatitis; and (4) alcohol intake < 20 g/day. Control liver tissues were obtained from adjacent non-lesional areas of age- and sex-matched patients undergoing surgical resection for hepatic hemangioma or elective cholecystectomy between April 2021 and December 2024. High-throughput RNA sequencing was performed on the biopsy samples using the Illumina NovaSeq 6000 platform, followed by comparative analysis of relative gene expression levels across samples. Histopathological evaluation was performed on liver biopsy specimens using the internationally established CRN (Kleiner) scoring system. The NAS was composed of three semi-quantitative components: steatosis (0–3), lobular inflammation (0–3), and hepatocellular ballooning (0–2), with a total score ranging from 0 to 8. MASLD was defined as the presence of any degree of hepatic steatosis. MASL (simple steatosis) was defined as steatosis ≥ 1, with lobular inflammation = 0 and hepatocellular ballooning = 0. MASH was diagnosed when steatosis ≥ 1, lobular inflammation ≥ 1, and hepatocellular ballooning ≥ 1 were present simultaneously.

Collection of gene expression profiles from the GEO database

Patients with MASLD were enrolled from three Japanese hospitals between 2014 and 2020. Eligible individuals fulfilled the Asian clinical criteria for MASLD [24]. For transcriptomic analysis, liver biopsy specimens were obtained from 98 patients with MASLD (MASL: 48; MASH: 50) at Sendai Kousei Hospital between 2016 and 2018. All samples were snap-frozen immediately after collection for global RNA sequencing. Histological diagnoses were confirmed by liver biopsy in all participants. Tissue specimens were paraffin-embedded, sectioned, and stained with hematoxylin and eosin and Masson's trichrome. All liver biopsies were centrally evaluated by a single experienced hepatopathologist using the NASH Clinical Research Network scoring system. Hepatic fibrosis was staged 0–4 according to the Kleiner classification, with advanced fibrosis defined as stage 3–4. Hepatic steatosis and lobular inflammation were graded 0–3, and hepatocellular ballooning 0–2. The NAS was calculated

as the sum of steatosis, lobular inflammation, and hepatocellular ballooning scores, with a range of 0–8.

A total of 59 human liver biopsy samples were obtained from a German cohort, comprising three phenotypic groups: controls ($n=27$), MASL ($n=14$), and MASH ($n=18$). All biopsies were rapidly frozen in liquid nitrogen to preserve RNA integrity [25]. Total RNA was isolated from homogenized liver tissue using the AllPrep DNA/RNA Mini Kit. Genome-wide mRNA expression analysis was performed using the HuGene 1.1 ST array platform. The transcriptomic datasets analyzed in this study are publicly accessible through the Gene Expression Omnibus (GEO) database, under the accession numbers GSE167523 (Japanese cohort) and GSE48452 (German cohort).

Statistical analysis

Continuous variables were summarized as means ± standard deviations (SD) or medians with interquartile ranges (IQR) depending on distribution normality, while categorical attributes were expressed as absolute frequencies and percentages. To evaluate baseline heterogeneity across MASL status, we employed Student's *t*-tests (or Mann–Whitney *U* tests) for continuous measures and Pearson's chi-squared tests for categorical data.

For the serum proteomic analysis, protein abundance was standardized to a mean of 0 and a standard deviation of 1. In the MRI cohort, serum proteins with < 97.5% detection were excluded, with missing values addressed via limit-of-detection (LOD) imputation and rank-based inverse normal transformation. Global proteomic variance across MRI-defined steatosis grades was quantified by PERMANOVA and visualized using PCoA. For model development, 1048 participants were partitioned (7:3 ratio) into discovery ($n=734$) and test ($n=314$) cohorts. Three algorithms (LightGBM, LASSO, and XGBoost) underwent tenfold cross-validation for feature selection, with predictive performance (AUC, sensitivity, specificity) assessed in the test dataset; AUCs were compared via DeLong's test. Feature importance was quantified using SHAP values, while protein-MASL associations were evaluated by generalized linear models (GLMs) adjusted for demographic and metabolic confounders. To identify serum protein signatures associated with longitudinal MASL incidence, baseline proteomic profiles were analyzed in relation to incident MASL diagnosed via serial ultrasonography. Candidate proteins identified by OPLS-DA (VIP > 1) were further prioritized using multivariable Cox regression to estimate adjusted hazard ratios (HRs). The reported *P* values were corrected for multiple testing via the Benjamini-Hochberg (BH) method, with significance defined at an FDR-adjusted $P<0.05$.

For the liver transcriptomic RNA-seq data, expression was normalized using Transcripts Per Million mapped reads (TPM). In the subsequent MASH cohort analysis, histopathological assessment (NAS scoring and CRN fibrosis staging) served as the gold standard for transcriptomic anchoring. We integrated a dual-methodology framework to identify robust gene signatures: random forest (RF) algorithms were employed for supervised feature selection to prioritize genes contributing to MASH and fibrosis progression, while linear modeling (limma) quantified differential expression across histological phenotypes. To assess the trans-ethnic generalizability of these hepatic gene signatures, we further validated our findings in independent Japanese and German liver transcriptomic datasets. The limma statistical framework and RF algorithms were employed in both cohorts to identify evolutionarily conserved MASH-associated gene signatures, thereby facilitating prioritization of biologically and therapeutically relevant targets. Multiple testing corrections were implemented using the Benjamini–Hochberg false discovery rate (FDR) method across all high-dimensional omics analyses. To investigate the interactions among the identified proteins, we constructed a protein–protein interaction network using the STRING (https://string-db.org/) [26]. The Gene Ontology (GO) enrichment methods provide insight at the gene set level for serum proteins and gene expression on the liver [27].

All statistical analyses were conducted using R statistical software, version 4.5.0 (R Foundation). A two-sided *P* value of less than 0.05 was considered to indicate statistical significance. The important R packages and resources were presented in Additional file 2: Table S1.

Results

Characteristics of the study population

The cross-sectional study of 1048 individuals (428 MASL and 620 non-MASL) diagnosed by MRI and a prospective study of 2945 individuals (1947 MASLD and 998 non-MASLD) assessed by ultrasonography were conducted. In the MRI cohort, the mean age was 56.84 ± 4.29 years, BMI 22.8 ± 3.00 kg/m^2, and approximately 70% were female (Additional file 2: Table S2). The prospective study had a mean age of 56.99 ± 4.80 years, BMI 21.95 ± 2.77 kg/m^2, and 64% female participants (Additional file 2: Table S3). Both studies showed statistically significant differences ($P<0.05$) in metabolic characteristics between MASL and non-MASL groups.

The study enrolled a total of 94 participants from the Zhejiang MASH cohort. The median age of the overall population was 54.00 years (IQR: 44.00, 68.00), with a balanced sex distribution of 49 males (52%) and 45 females (48%). According to histological assessment,

participants were stratified according to fibrosis stage: F0/1 ($n=36$, 38%), F2/3 ($n=47$, 50%), and F4 ($n=11$, 12%) (Additional file 2: Table S4). Patients were further classified into three NAS subgroups: NAS 0–2 ($n=12$, 13%), NAS 3–4 ($n=26$, 28%), and NAS ≥ 5 ($n=56$, 60%) (Additional file 2: Table S5). The validation cohort comprised 98 Japanese participants (median age 54.00 years; IQR 46.00–64.00), stratified by disease status into MASL ($n=48$) and MASH ($n=50$) groups (Additional file 2: Table S6). Conversely, the German cohort was younger, with a median age of 45.0 years (IQR: 38.0–50.0), and featured a marked female predominance (83%). Key clinical indicators recorded for the German population included BMI, fat percentage, adiponectin, and leptin levels, with the population categorized into healthy controls (46%), MASL (24%), and MASH (31%) (Additional file 2: Tables S7 and S8).

Association between serum proteins and hepatic steatosis severity

Liver fat content was assessed using MRI in 1048 participants from the MRI cohort. Based on metabolic factors, 428 participants were diagnosed with MASL (213 with mild MASL and 215 with moderate-to-severe MASL), and 620 were classified as healthy controls (Fig. 1A). PCoA based on PERMANOVA revealed a significant association between MASL severity and serum proteome variation ($R^2=22.14\%$) (Fig. 1B).

Analysis of an MRI cohort demonstrated that specific protein abundances vary significantly between healthy controls and individuals with mild or moderate-to-severe MASL (adjusted $P<0.05$) (Fig. 1C and D). Predictive modeling using machine learning algorithms of LightGBM further confirmed that these identified protein features can accurately distinguish MASL risk (AUC = 0.82), highlighting their potential as biomarkers for monitoring the severity of liver fat accumulation (Additional file 1: Fig. S3A and B). The protein–protein interaction (PPI) network analysis revealed strong interactions among AFM, C3, C9, F9, VTN, and SHBG (Additional file 1: Fig. S3C). Among the most significant findings, several complement and coagulation proteins, such as C3 (P01024), VTN (P04004), and CFH (P08603), as well as the liver-derived protein AFM (P43652), were positively correlated with increased MASL risk. Conversely, carrier and apolipoproteins including SHBG (P04278), APOD (P05090), and APOF (Q13790) exhibited a significant negative association, with levels decreasing as hepatic steatosis progressed (Fig. 1E, Additional file 2: Table S9).

Prospective associations between serum proteins and MASL incidence in ultrasound-defined participants

We further utilized a prospective population study to clarify the temporal relationship between serum proteomic signatures and MASL progression, while better controlling for confounding factors to strengthen the causal association between them. By integrating prospective study with ultrasound-based clinical assessments, this study has characterized a circulating protein signature associated with the risk and incidence of MASL. Within the prospective GNHS cohort (baseline $N=3415$), which featured a median follow-up of 9.8 years, proteomic profiles were utilized to distinguish participants who developed MASL from healthy controls (Fig. 2A). Differential abundance analysis and OPLS-DA modeling identified several candidate markers with high variable importance (VIP) scores (Fig. 2B), including proteins involved in the complement system and lipid metabolism. Specifically, baseline elevations in P43652 (AFM) and P04004 (VTN) were significantly associated with an increased hazard ratio (HR) for MASL incidence, while higher levels of Q13790 (APOF) and P04278 (SHBG) correlating with a lower risk of MASL (Fig. 2C). These findings were further validated by the significant downregulation of proteins such as Q13790 (APOF), P04278 (SHBG), and P05090 (APOD) in individuals with ultrasound-confirmed MASL compared to healthy controls, alongside the significant elevation of P43652 (AFM) (Fig. 2D, Additional file 2: Table S10).

Functional enrichment analysis revealed that serum proteins associated with MASL were primarily implicated in complement and coagulation cascades (Additional file 1: Fig. S4A–D).

Hepatic transcriptomic profiling

By integrating liver transcriptomic analysis with clinical grading, this study has identified critical gene expression signatures that distinguish severity of MASH and fibrosis. Differential expression analysis demonstrated that HMCN1 was significantly upregulated, while APOF was downregulated in patients with high NAS (NAS ≥ 3) compared to those with low NAS (Fig. 3A). Utilizing a random forest approach, the top 35 most influential features for predicting high NAS scores (NAS ≥ 3) were prioritized, with HMCN1, APOF, and RAD50, ITIH4 emerging as top-tier predictors (Fig. 3B), achieving stable model performance as indicated by the OOB error rate convergence (Fig. 3C). Furthermore, hierarchical clustering of these prioritized genes revealed distinct expression patterns that transitioned across NAS 0–2, 3–4, and ≥ 5 subgroups (Fig. 3D). Specifically, genes including C9, ITIH4,

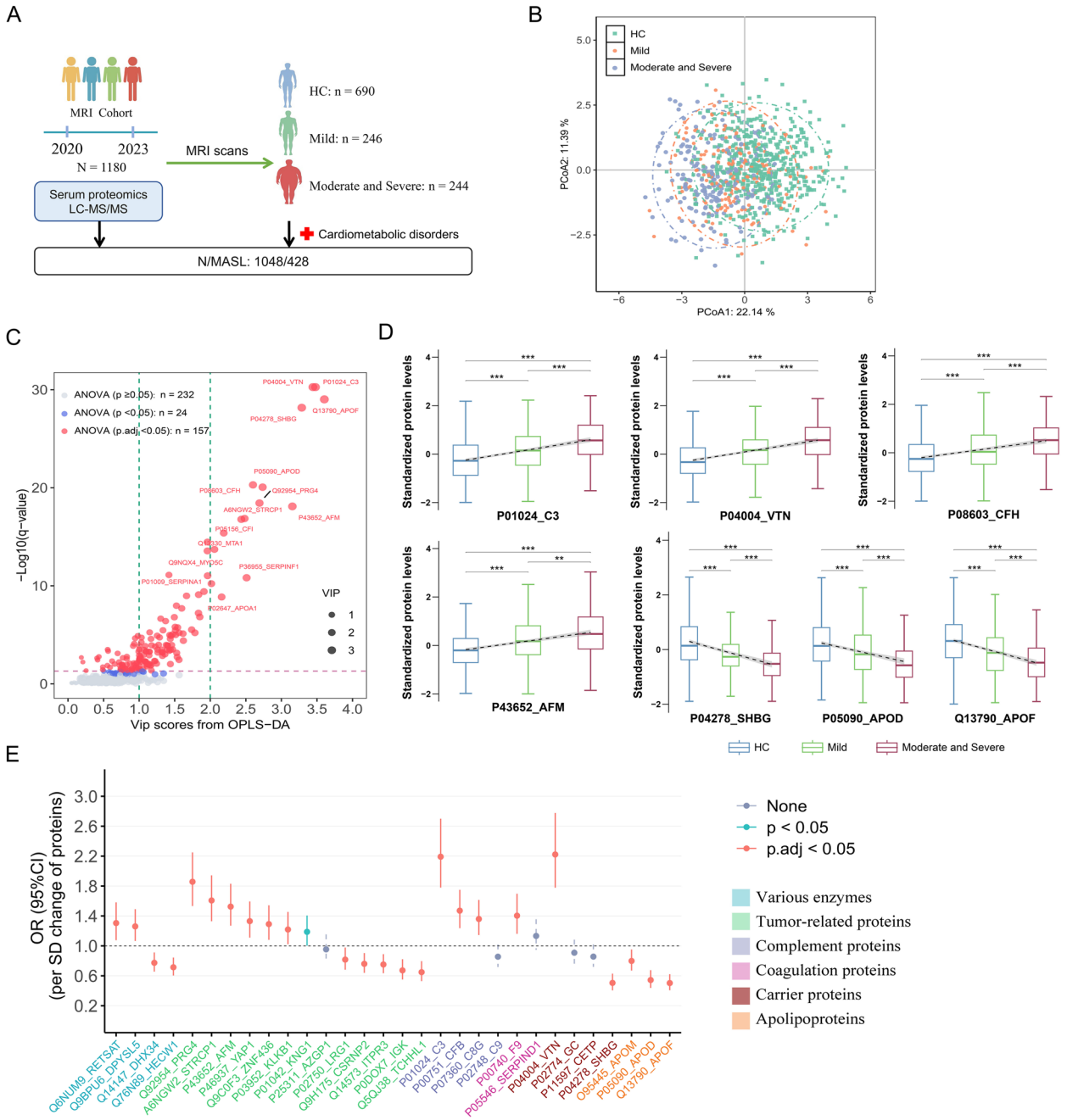

Fig. 1 Association between serum protein levels and MASL risk in MRI-defined participants. **A** Research design diagram; **B** principal coordinate analysis (PCoA) of serum proteomes across the three participant groups; **C** identification of serum proteins for hepatic steatosis grades; **D** box plots of significant serum proteins among different hepatic steatosis grades; **E** the forest plot of cross-sectional associations between protein features and MASL risk. Abbreviations: MASL, metabolic dysfunction-associated steatotic liver; MRI, magnetic resonance imaging; LC–MS/MS, liquid chromatography-tandem mass spectrometry; HC, healthy control; OPLS-DA, orthogonal partial least squares discriminant analysis; PCoA, principal coordinate analysis; ANOVA, analysis of variance; Vip, variable importance in projection; P.adj, adjusted *P* value by false discovery rate (*: $P < 0.05$; **: $P < 0.01$; ***: $P < 0.001$)

APOF, AFM, C4BPB, C1RL, HYDIN, APOL1, RAD50, HMCN1, TMEM185A, CHD8, and IQCG showed significant differential expression with increasing NAS grade, implying their potential roles as tissue-level markers of MASH progression. Functional enrichment analysis showed that dysregulated signatures were

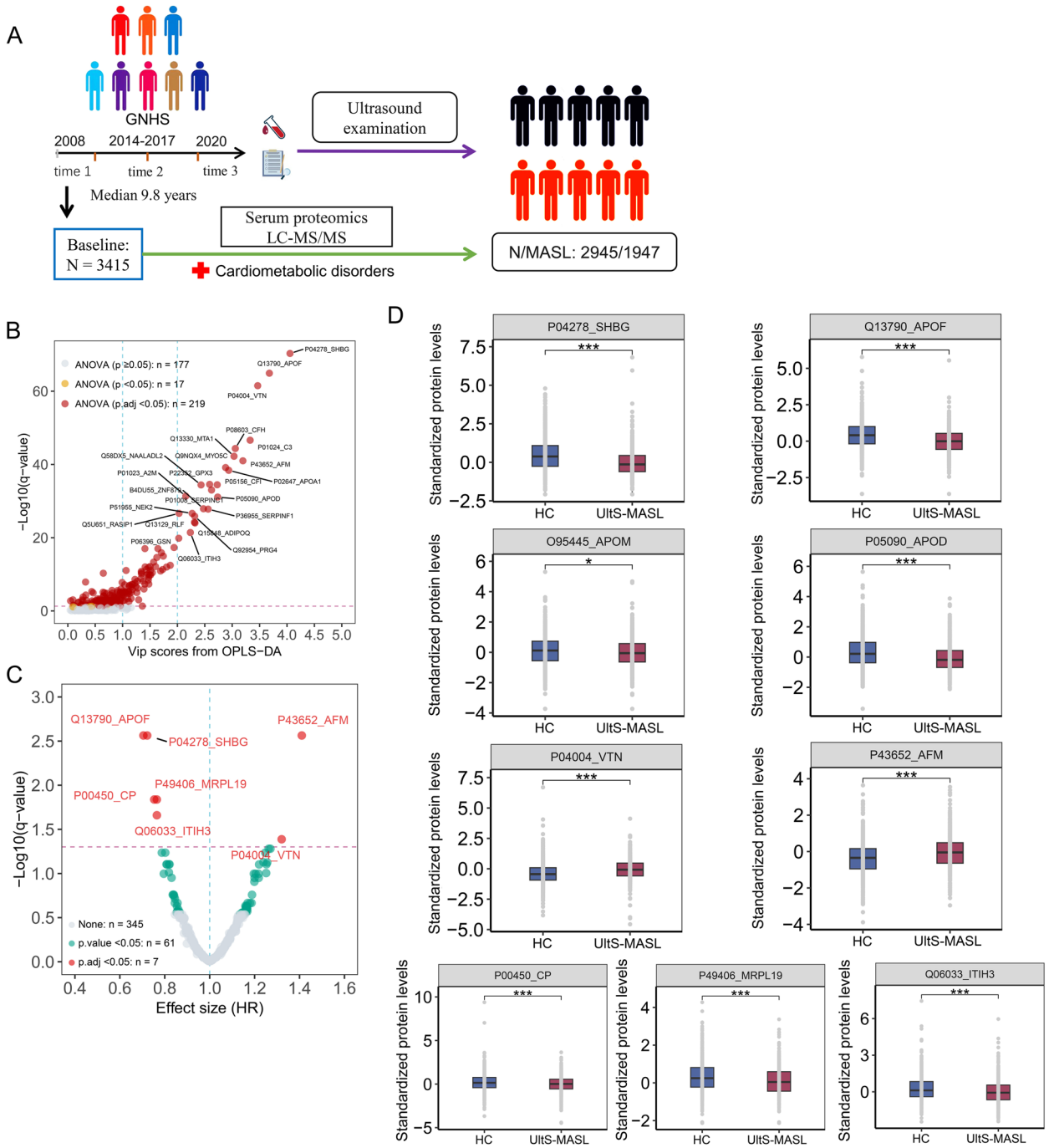

Fig. 2 Prospective associations between serum proteins and MASL incidence in ultrasound-defined participants. **A** Overview of the prospective study population; **B** identification of serum proteins for MASL incidence; **C** prospective associations between serum proteins and MASL incidence; **D** box plots illustrating protein expression differences between MASL and healthy controls (HC). Abbreviations: MASL, metabolic dysfunction-associated steatotic liver; MRI, magnetic resonance imaging; UltS, ultrasound; HC, healthy control; OPLS-DA, orthogonal partial least squares discriminant analysis; PCoA, principal coordinate analysis; ANOVA, analysis of variance; Vip, variable importance in projection; P.adj, adjusted *P* value by false discovery rate (*: $P < 0.05$; **: $P < 0.01$; ***: $P < 0.001$)

mainly involved in three biological processes: complement-mediated immune regulation, lipid homeostasis, and protease inhibition. Genes including C9, C1RL, C4BPB, and APCS were significantly enriched in innate immune response pathways, particularly complement activation and blood microparticle formation. APOF

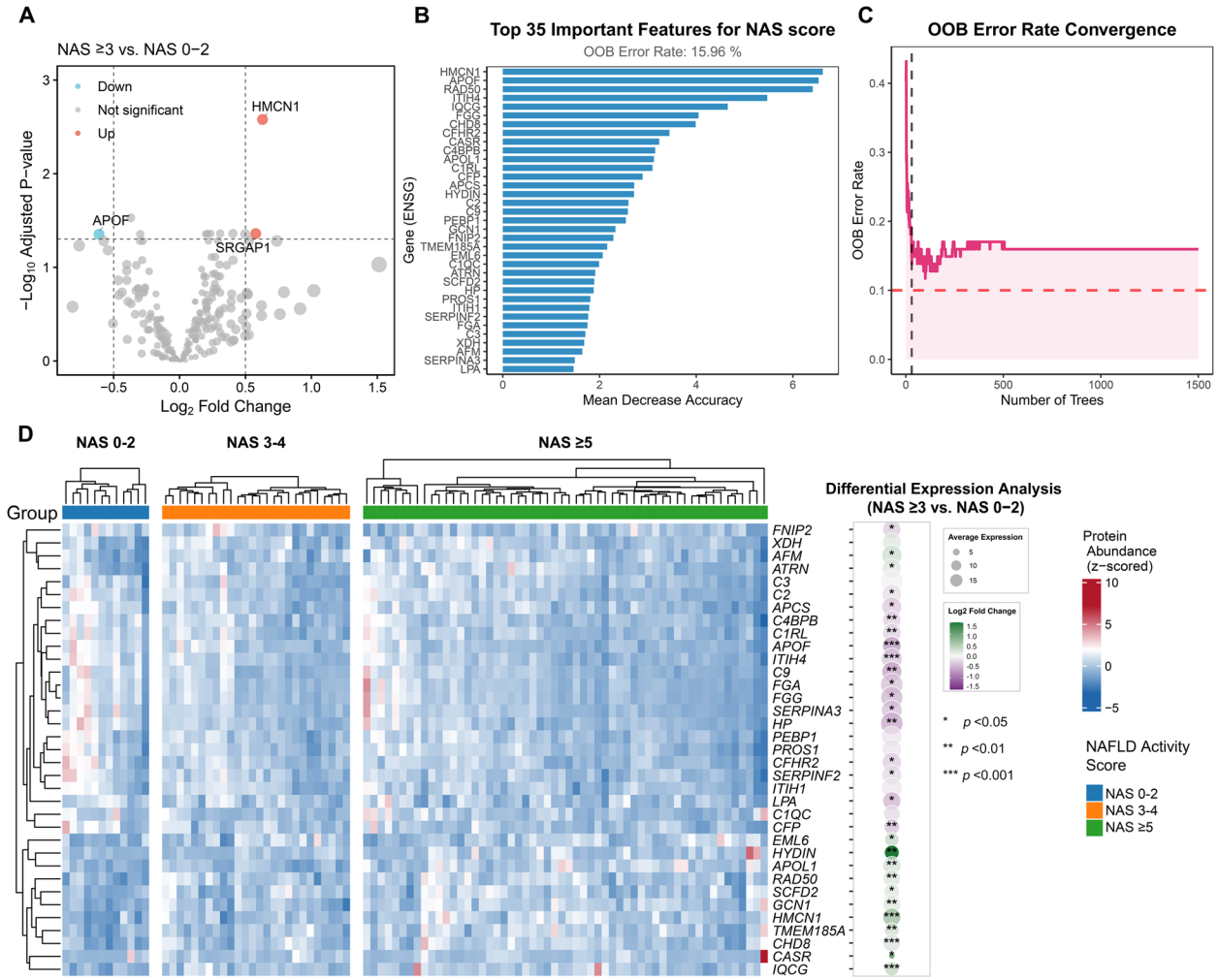

Fig. 3 Transcriptomic signatures associated with NAFLD Activity Score (NAS) in liver of Han population. **A** Volcano plot of differentially expressed genes between the higher and lower NAS groups (NAS ≥ 3 vs. NAS 0–2); **B** selection of key genes for higher NAS by random forest model; **C** in-bag error curve for determining optimal number of gene features in random forest model; **D** heatmap of expression patterns of NAS-associated gene features across different NAS grades. Abbreviations: NAFLD, non-alcoholic fatty liver disease; NAS, NAFLD Activity Score; MASH, metabolic dysfunction-associated steatohepatitis

and APOL1 participated in high-density lipoprotein structural stability and lipid transport, whereas ITIH4, SERPINA3, and AFM were associated with endopeptidase inhibitor activity and acute inflammatory response in secretory granule and vesicle lumens (Additional file 1: Fig. S5).

Principal component analysis demonstrated that global liver gene expression patterns significantly diverged as fibrosis progressed from F0/1 to F4 stages (Fig. 4A). Differential expression analysis between advanced fibrosis (F2–4) and early stages (F0/1) revealed a marked upregulation of genes such as A2M, LUM, and C7, while IGFALS was significantly downregulated (Fig. 4B). These trends were further confirmed by stage-specific expression analysis, where genes like A2M, GSN, and LUM exhibited a progressive increase across F0/1, F2/3, and F4 categories (Fig. 4C and D). Utilizing a random forest algorithm, the top 40 most influential genetic features for fibrosis prediction were prioritized (Additional file 1: Fig. S6A and B), achieving high classification accuracy with an AUC of 0.97 (Additional file 1: Fig. S6C and D). Hierarchical clustering and z-scored abundance maps further illustrated that these prioritized proteins, including CHST4, GSN, C7, LUM, A2M, SHBG, and IGFALS, were distinctly repressed in advanced fibrosis (Fig. 4E). Functional enrichment analysis through a Sankey diagram linked these candidate proteins to critical biological pathways,

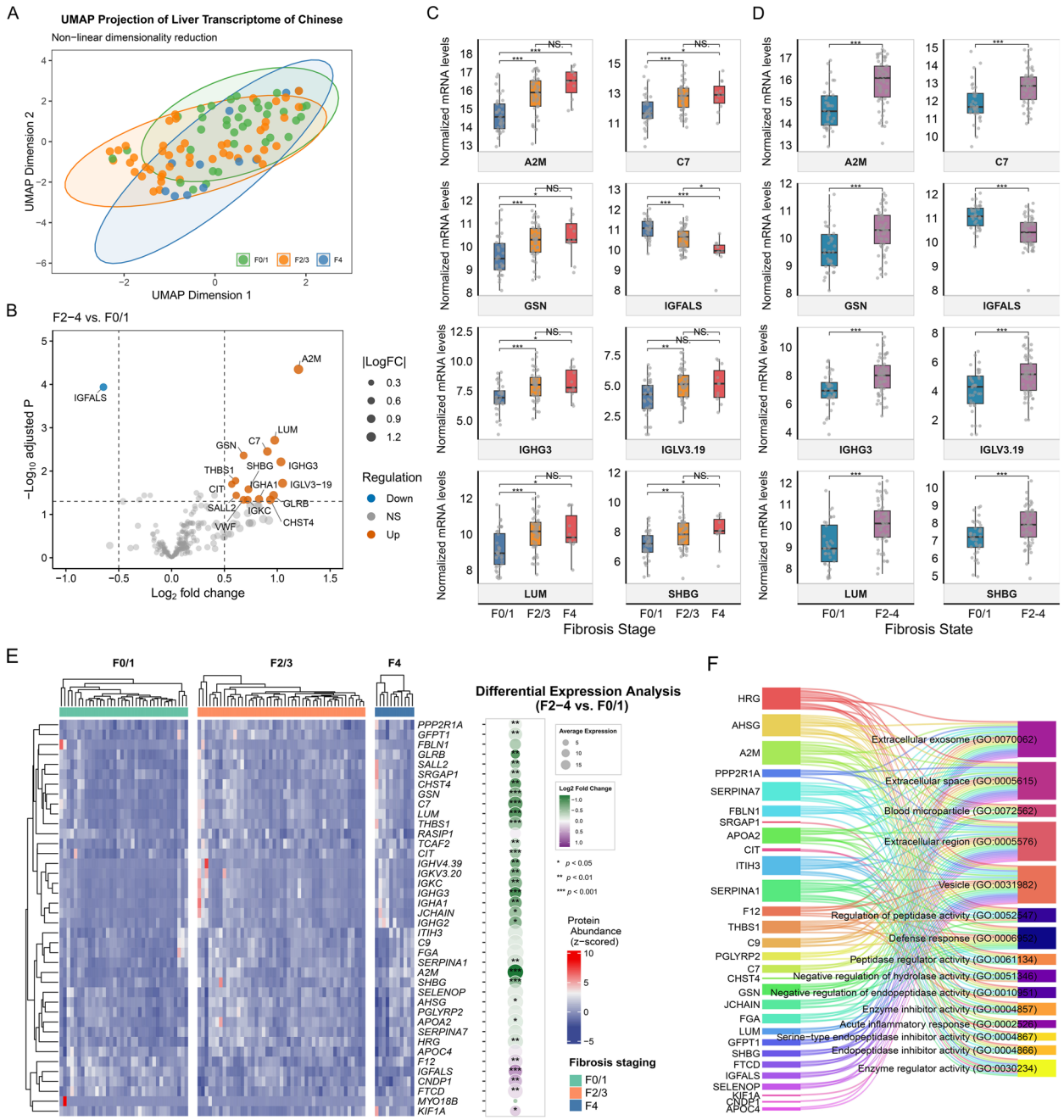

Fig. 4 Transcriptomic signatures associated with liver fibrosis stages based on CRN score. **A** Uniform manifold approximation and projection (UMAP) plot of the global transcriptome profiles across liver samples, color-coded by CRN-based fibrosis stages (F0–1, F2–3, F4); **B** volcano plot identifying differentially expressed genes (DEGs) associated with advanced fibrosis; **C**, **D** box plots showing the expression levels of selected genes across different liver fibrosis stages (F0–1, F2–3, F4); **E** heatmap displaying the expression patterns of the selected fibrosis-associated gene signatures across samples stratified by CRN-based fibrosis stages (F0–1, F2–3, F4); **F** Sankey diagram illustrating the Gene Ontology (GO) functional enrichment pathways of the key fibrosis-related gene signatures, linking genes to their enriched biological processes (*: $P < 0.05$; **: $P < 0.01$; ***: $P < 0.001$)

particularly the extracellular exosome, extracellular space, blood microparticle, extracellular region, and vesicle (Fig. 4F).

To validate disease-associated molecular signatures, liver transcriptomic analysis was performed on a Japanese cohort (overall, $n = 98$; MASL, $n = 48$; MASH,

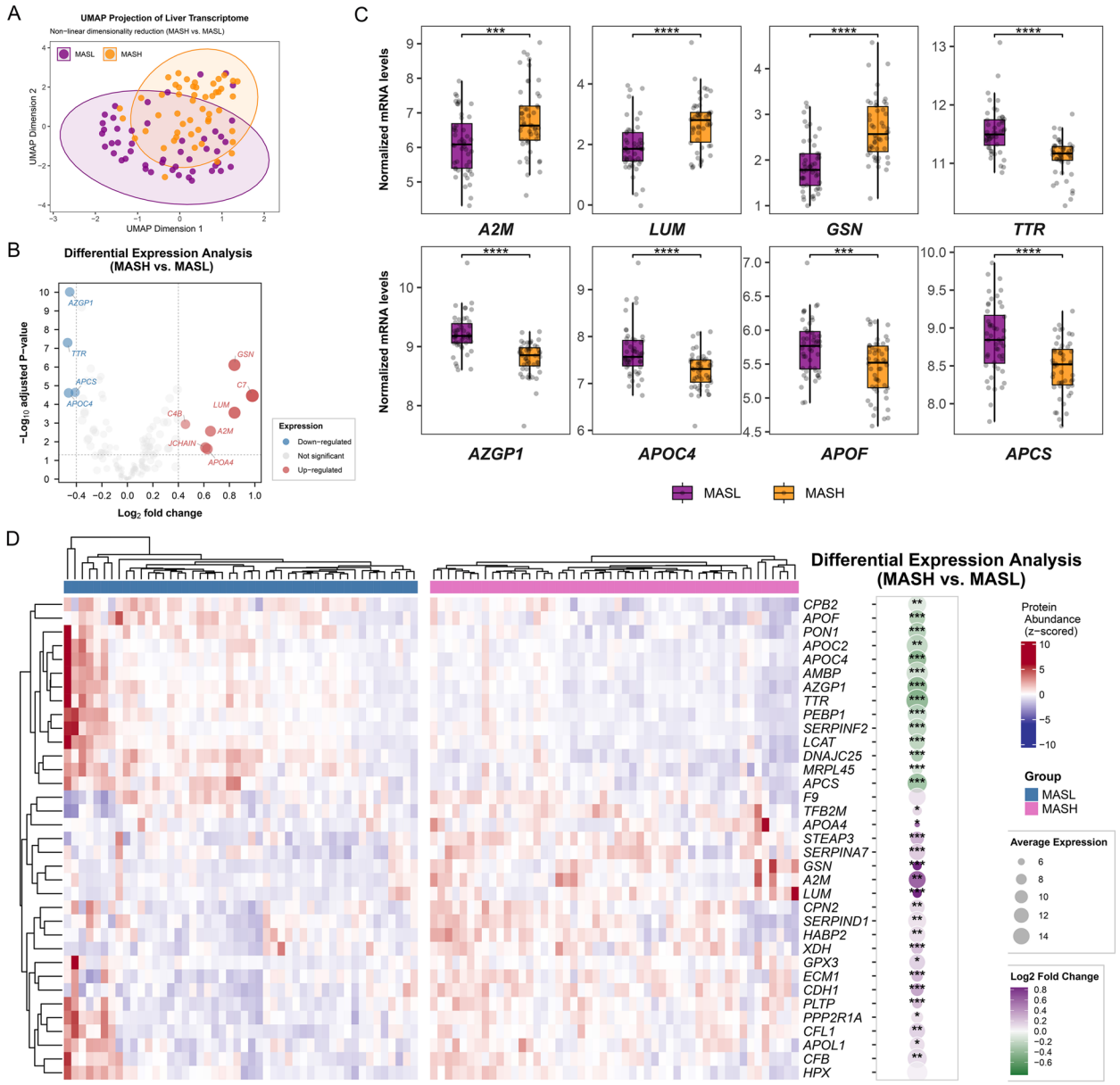

Fig. 5 Transcriptomic profiling reveals distinct molecular signatures between MASH and MASL in Japanese liver tissue. **A** The UMAP plot of liver transcriptome data showing non-linear dimensionality reduction of global gene expression profiles between MASL (purple) and MASH (orange) samples. The ellipses indicate 95% confidence intervals for each group distribution, demonstrating clear separation between the two disease stages; **B** volcano plot illustrating differentially expressed mRNAs between MASH and MASL identified by limma analysis. The x-axis represents $\log_2$ fold change, and the y-axis represents $-\log_{10}$ adjusted *P* value; **C** box plots displaying normalized mRNA expression levels of representative differentially expressed genes between MASL (purple) and MASH (orange) groups; **D** hierarchical clustering heatmap of differentially expressed mRNAs between MASH and MASL samples (*: $P<0.05$; **: $P<0.01$; ***: $P<0.001$; ****: $P<0.0001$)

$n=50$). UMAP projection revealed a distinct separation between MASL and MASH groups, reflecting a significant global mRNA profile shift during the transition to steatohepatitis (Fig. 5A). Differential expression analysis identified numerous significant mRNAs in MASH patients, characterized by the upregulation of genes involved in extracellular matrix remodeling and inflammation (A2M, LUM, and GSN) and the downregulation of those associated with lipid metabolism and hepatocyte functions (TTR, AZGP1, APOC4, APOF, and APCS (Fig. 5B–D).

To identify robust molecular markers distinguishing MASH from MASL, a random forest algorithm was applied to the Japanese validation cohort, identifying the

top 35 transcriptomic features with a stable out-of-bag (OOB) error rate of 16.33%. According to mean decrease accuracy, CFL1, AZGP1, DNAJC25, and GSN served as the primary genes (Additional file 1: Fig. S7A and B). Functional enrichment analysis demonstrated that these signatures were predominantly involved in lipid metabolism and transport, including high-density lipoprotein particles, cholesterol transport, and protein-lipid complex remodeling. Additionally, genes including A2M and SERPINF2 were associated with serine-type endopeptidase and enzyme inhibitor activity, whereas others were linked to complement binding, suggesting coordinated dysregulation of inflammation and extracellular proteolysis during MASH progression (Additional file 1: Fig. S7C).

In an independent validation involving the German population, hepatic transcriptomic analysis confirmed the downregulation of key metabolic regulators and the upregulation of structural proteins in relation to MASH. Differential expression analysis revealed that APOF, C9, KLKB1, and PZP were significantly downregulated in patients with higher NAS (NAS ≥ 3) and MASH status

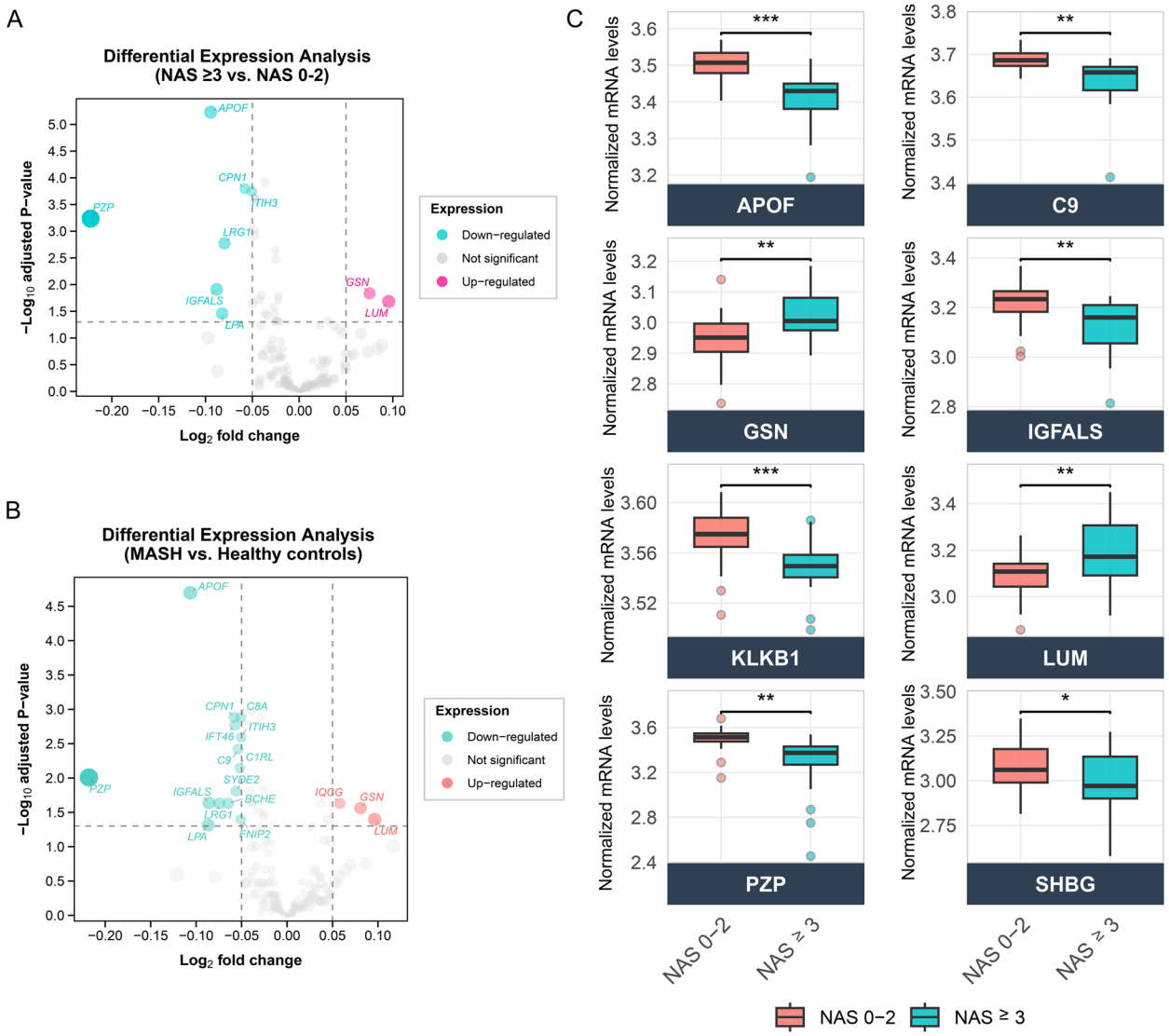

Fig. 6 Transcriptomic signatures associated with NAFLD Activity Score (NAS) in liver of German population. **A** Volcano plot of differentially expressed genes between the higher and lower NAS groups (NAS ≥ 3 vs. NAS 0–2); **B** volcano plot of differentially expressed genes between MASH and healthy controls; **C** box plots illustrating protein expression differences between the higher and lower NAS groups (NAS ≥ 3 vs. NAS 0–2). Abbreviations: NAFLD, non-alcoholic fatty liver disease; NAS, NAFLD Activity Score; MASH, metabolic dysfunction-associated steatohepatitis (*: $P < 0.05$; **: $P < 0.01$; ***: $P < 0.001$)

compared to healthy or low NAS (Fig. 6A and B). Conversely, genes such as GSN and LUM exhibited significant upregulation in advanced disease states (Fig. 6A and B). These findings were corroborated by stage-specific expression levels, where APOF, C9, KLKB1, PZP, IGFALS, and SHBG showed markedly reduced expression in the NAS ≥ 3 subgroup, while GSN and LUM levels were significantly elevated (Fig. 6C).

Discussion

By integrating serum proteomics from independent cohorts with liver transcriptomics from a separate clinical collective, we extended systemic protein findings into the intrahepatic domain, refining our understanding of MASLD through the lens of local transcriptional remodeling and its associated molecular architecture. The serum proteomics analysis found that elevated complement/acute-phase proteins (C3, C9, VTN, AFM) and decreased metabolic regulators (SHBG, APOF) were linked to the risk of MASL. Transcriptomic analysis of liver further demonstrated that these circulating disturbances were mirrored within the hepatic microenvironment, where downregulation of complement inhibitors (C9, C4BPB, C1RL, ITIH4) and metabolic genes (APOF) marks the progression to high NAS. Additionally, advanced fibrosis is defined by a shift toward extracellular matrix remodeling, evidenced by upregulation of structural proteins (GSN and LUM) and downregulation of hepatoprotective factors (IGFALS, SHBG).

Our serum proteomic analysis identified a panel of proteins, including AFM, VTN, C3, and C9, that are significantly associated with MASL risk. Afamin (AFM) is a member of the albumin family and was positively related with NAFLD as a pleiotropic glycoprotein [12]. The serum afamin level was used to predict the risk of gestational diabetes and preeclampsia, and afamin levels in obese patients may be involved in the development of obesity-associated oxidative stress through insulin resistance [28]. The study found serum afamin may be a novel marker of increased hepatic lipid content [29, 30]. Vitronectin (VTN) is a glycoprotein involved in cell adhesion and the regulation of the complement system [31]. The previous study showed a 22% increase of VTN in NAFLD patients and identified a panel of three proteins (PIGR, ALDOB, and VTN) related to NAFLD without T2DM [12]. Meanwhile, the component proteins, SHBG and apolipoproteins (APOF, APOE, APOC1, APOB, and APOA), were found to be associated with fatty liver [32]. Apolipoprotein F (APOF) is a natural inhibitor of cholesteryl ester transfer protein and a key regulator of lipoprotein metabolism that was reduced in humans with steatosis and controls plasma triglyceride-rich lipoprotein metabolism [33]. Decreased expression of APOF was associated with poor prognosis in human hepatocellular carcinoma [34]. Sex hormone-binding globulin (SHBG) binds to sex hormones like testosterone and estradiol, regulating their bioavailability [35]. Lower levels of SHBG in young men are associated with increase in prevalent MASLD in middle age [35].

A coordinated downregulation of hepatic transcripts, including C3, C2, C4BPB, C1RL, and APOF, was observed in patients with high NAS score. Conversely, serum levels of complement components C3 and C9 were elevated during early steatosis, indicative of systemic low-grade inflammation [36]. This dissociation has suggested that active hepatic inflammation in MASH may involve local consumption or feedback suppression of complement-related gene expression, marking a critical shift in pathophysiology [37]. Furthermore, the reduced expression of ITIH4 and AFM in MASH-affected liver tissue has implied a diminished protective response against inflammatory stress [38]. Such dysregulation within the complement cascade has supported the view that MASH represents a distinct immunological transition rather than a simple escalation of steatosis, underscoring the role of innate immunity in hepatocyte injury [39]. Our analysis identified significant intrahepatic upregulation of genes involved in tissue remodeling, specifically complement C7 (C7), alpha-2-macroglobulin (A2M), gelsolin (GSN), and lumican (LUM), all of which showed a progressive increase corresponding to the severity of liver fibrosis. Reflecting the molecular patterns identified in established MASH cohorts, we observed that the expression of C7, A2M, and LUM increases progressively with advancing fibrosis stages. These findings suggest that as the disease moves beyond MASH, the hepatic molecular environment undergoes a profound transformation, prioritize inflammatory signaling and structural remodeling [24]. Lumican, a leucine-rich proteoglycan essential for collagen fibrillogenesis, was consistently elevated in both Chinese and European cohorts, confirming its utility as a reliable marker of fibrotic severity [40].

Functional analysis has further linked these markers to extracellular vesicle pathways, suggesting that fibrotic livers may release protein-carrying vesicles that mediate systemic communication. Our results are corroborated by a study of 318 NAFLD patients, in which the reported perturbations in inflammatory, complement, and coagulation pathways parallel the systemic proteomic signatures and intrahepatic shifts observed in our analysis [41]. Additionally, the downregulation of IGFALS and SHBG in advanced fibrosis has indicated a suppression of the growth hormone-IGF-1 axis, which may underlie the metabolic dysfunction and sarcopenia observed in progressive disease [42]. Based on the observational study findings, a discordance exists

between serum proteins associated with simple MASL and hepatic transcriptional genes linked to MASH and liver fibrosis which may reflect the complex regulatory landscape of advanced liver disease. The observed divergence suggests a decoupling between hepatic transcription and protein secretion. While compensatory mRNA upregulation persists under cellular stress, MASH-associated endoplasmic reticulum (ER) stress may impair secretory pathways, reducing circulating protein output [43]. Moreover, unlike the liver-localized transcriptome, the serum proteome integrates multi-organ crosstalk; systemic insulin resistance and inflammation drive extrahepatic contributions that confound liver-derived signals [44]. Consequently, systemic protein alterations primarily reflect early metabolic shifts in MASL, whereas hepatic transcriptional profiles capture the progression toward inflammation and fibrosis in MASH [45]. RNA-seq outperforms microarrays by providing enhanced sensitivity and a broader dynamic range while circumventing the inherent constraints of probe-based hybridization.

Several limitations should be considered when interpreting the results of this study. First, despite cross-ethnic validation using a Japanese hepatic transcriptomic cohort, all main study populations were of Asian ancestry, which may limit the generalizability of our findings to other ethnic and geographic groups. Second, serum proteomic and liver transcriptomic analyses were performed in independent cohorts without overlap, preventing direct paired comparisons between circulating protein levels and hepatic mRNA expression in the same individuals. Third, the observed associations are descriptive and do not establish causality; further functional experiments are needed to validate the biological roles and mechanisms of the identified signatures during MASLD progression.

Conclusions

In conclusion, these results delineate a model wherein systemic proteomic changes align with hepatic transcriptional reprogramming to drive progression from steatosis to inflammation and fibrosis. Proteins such as AFM, APOF, SHBG, LUM, and GSN improve the understanding of MASLD and represent potential stage-specific biomarkers and therapeutic targets. Early disease involves lipid transport and metabolic alterations, whereas progression is linked to complement dysregulation and extracellular matrix remodeling. Consistently validated across cohorts, these proteins offer translational promise for drug development and noninvasive monitoring. These findings provide a mechanistic rationale for therapeutic targeting. Future work should prioritize functional validation and clinical translation.

Abbreviations

DBP	Diastolic blood pressure
FDR	False discovery rate
HC	Hip circumference
HDL-C	High-density lipoprotein cholesterol
HR	Hazard ratio
LDL-C	Low-density lipoprotein cholesterol
MASLD	Metabolic dysfunction-associated steatotic liver disease
MASH	Metabolic dysfunction-associated steatohepatitis
MRI	Magnetic resonance imaging
NAFLD	Non-alcoholic fatty liver disease
SBP	Systolic blood pressure
TC	Total cholesterol
TG	Triglyceride
WHR	Waist-to-hip ratio
LC–MS/MS	Liquid chromatography-mass spectrometry
LightGBM	Light Gradient Boosting Machine
UltS	Ultrasonography
WC	Waist circumference

Supplementary Information

The online version contains supplementary material available at https://doi.org/10.1186/s12916-026-04834-8.

Additional file 1: Supplementary Figures S1–S7 and supplementary methods. Figure S1. The flowchart for inclusion and exclusion of study subjects. Figure S2. The definition of MASLD. Figure S3. Selection of serum protein features for MASL risk based on machine learning algorithms. Figure S4. The functional enrichment of serum proteins associated with MASL risk. Figure S5. Functional GO enrichment analysis of differentially expressed mRNAs in patients with high NAS (NAS ≥2) within the Zhejiang MASH cohort. Figure S6. Selection of liver fibrosis-related hepatic transcriptional gene features based on a random forest model. Figure S7. Differential hepatic transcriptomic signatures distinguishing MASH from MASL in a Japanese cohort identified via random forest modeling. Supplementary methods: Method 1. Questionnaire interview and laboratory assays. Method 2. The diagnostic criteria of MASLD. Method 3. Circulating proteome profiling. Method 4. Data quality control (QC) of proteome data.

Additional file 2: Supplementary Tables S1–S10. Table S1. Key resources table. Table S2. General characteristics of the study participants based on abdominal magnetic resonance imaging. Table S3. Baseline characteristics of study participants based on abdominal ultrasound. Table S4. Characteristics of study subjects by liver fibrosis stages in the Zhejiang MASH cohort. Table S5. Characteristics of participants by NAFLD activity score levels in the Zhejiang MASH cohort. Table S6. Characteristics of participants across disease status in the Japanese population. Table S7. Characteristics of participants according to NAS levels in the German population. Table S8. Characteristics of participants across disease status in the German population. Table S9. The correlation between serum proteins and the risk of MASL diagnosed by MRI. Table S10. The correlation between serum proteins and the risk of MASL detected by ultrasound diagnosis.

Acknowledgements

The authors would like to thank all participants who were included in providing the data. We would like to thank Westlake University Supercomputer Centre for assistance in data storage and computation. We thank the support from Westlake Education Foundation and Westlake Intelligent Biomarker Discovery Lab at the Westlake Laboratory of Life Sciences and Biomedicine. We thank the group of Professor Tetsuo Takehara from the Department of Gastroenterology and Hepatology, Osaka University Graduate School of Medicine, and Professor Jochen Hampe's team from the Department of General and Thoracic Surgery, Christian-Albrechts-University Kiel/University Hospital Schleswig-Holstein, for sharing the hepatic transcriptomic and phenotypic datasets deposited in the Gene Expression Omnibus (GEO).

Authors' contributions

Study conception and design: Y.M.C., J.S.Z. Data analysis and manuscript drafting: J.J.X., W.L.G., X.Y.W. Interpretation of the results and critical review of the manuscript: Y.M.C., J.S.Z., J.J.X., W.L.G., X.Y.W., D.M.R., W.H., J.T.C., B.Y.L., Y.X. All

authors provided comments and critical revisions on drafts of the manuscript. All authors read and approved the final manuscript.

Funding
This study was jointly supported by the National Natural Science Foundation of China (82574079 and 82073546 to Y.-M.C. and 82073529 to J.-S.Z.); Zhejiang Provincial Health Industry Science and Technology Program (2025HY0058 to J.J.X.); the Key Research and Development Program of Guangdong Province, China (2019B20227003 to Y.-M.C.); and the 5010 Program for Clinical Researches of the Sun Yat-sen University (Guangzhou, China) (2007032 to Y.-M.C.).

Data availability
The mass spectrometry proteomics data have been deposited to the ProteomeXchange Consortium (http://proteomecentral.proteomexchange.org) via the iProX partner repository with the dataset identifier PXD039236, PXD039231, and PXD038253. The phenotype data and any additional information required to reanalyze the data reported in this work paper is available from the lead contact and the first author. The transcriptomic datasets for the Japanese and German cohorts are publicly available from the Gene Expression Omnibus (GEO) repository (https://www.ncbi.nlm.nih.gov/geo/) under accession numbers GSE167523 (Japanese cohort) and GSE48452 (German cohort).

Declarations

Ethics approval and consent to participate
The present study was performed in accordance with the Declaration of Helsinki. The protocol of the Guangzhou Nutrition and Health Study was approved by the Institutional Review Board of the School of Public Health, Sun Yat-sen University (No. SYSU-2018–048). Ethical approval for participant enrollment and biosample collection was granted by the Institutional Review Board of Zhejiang Provincial People's Hospital (No. 2021KY044). Written informed consent was obtained from all participants before study inclusion.

Consent for publication
Not applicable.

Competing interests
The authors declare no competing interests.

Author details
[1]Department of Endocrinology, Key Laboratory of Endocrine Gland Diseases of Zhejiang Province, Geriatric Medicine Center, Zhejiang Provincial People's Hospital (Affiliated People's Hospital, Hangzhou Medical College), Hangzhou 310014, China. [2]Department of Epidemiology, Guangdong Provincial Key Laboratory of Food, Nutrition and Health, School of Public Health, Sun Yat-Sen University, Guangzhou 510275, China. [3]School of Future Biomedicine and School of Life Sciences, Westlake University, Hangzhou 310030, China. [4]School of Medicine, Westlake University, Hangzhou 310030, China.

Received: 31 December 2025 Accepted: 25 March 2026
Published online: 17 April 2026

References

1. Tilg H, Petta S, Stefan N, Targher G, Niu L, Thiele M, et al. Metabolic dysfunction-associated steatotic liver disease in adults: a review non-invasive proteomic biomarkers for alcohol-related liver disease. JAMA. 2025;28:1277–87.
2. Orci LA, Sanduzzi-Zamparelli M, Caballol B, Sapena V, Colucci N, Torres F, et al. Incidence of hepatocellular carcinoma in patients with nonalcoholic fatty liver disease: a systematic review, meta-analysis, and meta-regression. Clin Gastroenterol Hepatol. 2022;20:283-292.e210.
3. Mantovani A, Petracca G, Beatrice G, Csermely A, Tilg H, Byrne CD, et al. Non-alcoholic fatty liver disease and increased risk of incident extrahepatic cancers: a meta-analysis of observational cohort studies. Gut. 2022;71:778–88.
4. Jara M, Norlin J, Kjær MS, Almholt K, Bendtsen KM, Bugianesi E, et al. Modulation of metabolic, inflammatory and fibrotic pathways by semaglutide in metabolic dysfunction-associated steatohepatitis. Nat Med. 2025;31:3128–40.
5. Yao P, Iona A, Pozarickij A, Said S, Wright N, Lin K, et al. Proteomic analyses in diverse populations improved risk prediction and identified new drug targets for type 2 diabetes. Diabetes Care. 2024;47:1012–9.
6. Abozaid YJ, Ayada I, van Kleef LA, Vallerga CL, Pan Q, Brouwer WP, et al. Plasma proteomic signature of fatty liver disease: the Rotterdam Study. Hepatology. 2023;78:284–94.
7. Liu WS, You J, Chen SD, Zhang Y, Feng JF, Xu YM, et al. Plasma proteomics identify biomarkers and undulating changes of brain aging. Nat Aging. 2025;5:99–112.
8. Oh HS, Le Guen Y, Rappoport N, Urey DY, Farinas A, Rutledge J, et al. Plasma proteomics links brain and immune system aging with healthspan and longevity. Nat Med. 2025;31:2703–11.
9. Liu J, Xiao S, Hu S, Huang R, Chen L, Tomlinson JW, et al. Dissecting metabolic dysfunction- and alcohol-associated liver disease (MetALD) using proteomic and metabolomic profiles. J Hepatol. 2025;83:1035–45.
10. De Nardo W, Lee O, Johari Y, Bayliss J, Pensa M, Miotto PM, et al. Integrated liver-secreted and plasma proteomics identify a predictive model that stratifies MASH. Cell Rep Med. 2025;6:102085.
11. Sanyal AJ, Williams SA, Lavine JE, Neuschwander-Tetri BA, Alexander L, Ostroff R, et al. Defining the serum proteomic signature of hepatic steatosis, inflammation, ballooning and fibrosis in non-alcoholic fatty liver disease. J Hepatol. 2023;78:693–703.
12. Niu L, Geyer PE, Wewer Albrechtsen NJ, Gluud LL, Santos A, Doll S, et al. Plasma proteome profiling discovers novel proteins associated with non-alcoholic fatty liver disease. Mol Syst Biol. 2019;15:e8793.
13. Sveinbjornsson G, Ulfarsson MO, Thorolfsdottir RB, Jonsson BA, Einarsson E, Gunnlaugsson G, et al. Multiomics study of nonalcoholic fatty liver disease. Nat Genet. 2022;54:1652–63.
14. Stefanakis K, Mingrone G, George J, Mantzoros CS. Accurate non-invasive detection of MASH with fibrosis F2-F3 using a lightweight machine learning model with minimal clinical and metabolomic variables. Metabolism. 2025;163:156082.
15. Zhang S, Xu H, Li M, Yuan G, Nie J, Zhang Q, et al. An etiology-stratified single-cell atlas identifies FABP4 as a prognostic marker for MASLD-related HCC. J Hepatol. 2025. https://doi.org/10.1016/j.jhep.2025.10.026.
16. Ling CW, Zhong H, Zeng FF, Chen G, Fu Y, Wang C, et al. Cohort profile: Guangzhou Nutrition and Health Study (GNHS): a population-based multi-omics study. J Epidemiol. 2023;34:301–6.
17. Tamaki N, Ajmera V, Loomba R. Non-invasive methods for imaging hepatic steatosis and their clinical importance in NAFLD. Nat Rev Endocrinol. 2022;18:55–66.
18. Loomba R, Adams LA. Advances in non-invasive assessment of hepatic fibrosis. Gut. 2020;69:1343–52.
19. Gu J, Liu S, Du S, Zhang Q, Xiao J, Dong Q, et al. Diagnostic value of MRI-PDFF for hepatic steatosis in patients with non-alcoholic fatty liver disease: a meta-analysis. Eur Radiol. 2019;29:3564–73.
20. Castera L, Friedrich-Rust M, Loomba R. Noninvasive assessment of liver disease in patients with nonalcoholic fatty liver disease. Gastroenterology. 2019;156:1264-1281.e1264.
21. Chalasani N, Younossi Z, Lavine JE, Charlton M, Cusi K, Rinella M, et al. The diagnosis and management of nonalcoholic fatty liver disease: practice guidance from the American Association for the Study of Liver Diseases. Hepatology. 2018;67:328–57.
22. Rinella ME, Lazarus JV, Ratziu V, Francque SM, Sanyal AJ, Kanwal F, et al. A multisociety Delphi consensus statement on new fatty liver disease nomenclature. J Hepatol. 2023;79:1542–56.
23. Tang M, Huang P, Wu L, Zhou P, Gong P, Liu X, et al. Comprehensive evaluation and optimization of the data-dependent LC-MS/MS workflow for deep proteome profiling. Anal Chem. 2023;95:7897–905.
24. Kozumi K, Kodama T, Murai H, Sakane S, Govaere O, Cockell S, et al. Transcriptomics identify thrombospondin-2 as a biomarker for NASH and advanced liver fibrosis. Hepatology. 2021;74:2452–66.
25. Ahrens M, Ammerpohl O, von Schönfels W, Kolarova J, Bens S, Itzel T, et al. DNA methylation analysis in nonalcoholic fatty liver disease suggests distinct disease-specific and remodeling signatures after bariatric surgery. Cell Metab. 2013;18:296–302.
26. Zhao N, Zhuo M, Tian K, Gong X. Protein-protein interaction and non-interaction predictions using gene sequence natural vector. Commun Biol. 2022;5:652.

27. Ietswaart R, Gyori BM, Bachman JA, Sorger PK, Churchman LS. GeneWalk identifies relevant gene functions for a biological context using network representation learning. Genome Biol. 2021;22:55.
28. Yuan Y, He W, Fan X, Liang J, Cao Z, Li L. Serum afamin levels in predicting gestational diabetes mellitus and preeclampsia: a systematic review and meta-analysis. Front Endocrinol (Lausanne). 2023;14:1157114.
29. Kurdiova T, Balaz M, Kovanicova Z, Zemkova E, Kuzma M, Belan V, et al. Serum afamin a novel marker of increased hepatic lipid content. Front Endocrinol (Lausanne). 2021;12:670425.
30. Pitkänen N, Finkenstedt A, Lamina C, Juonala M, Kähönen M, Mäkelä KM, et al. Afamin predicts the prevalence and incidence of nonalcoholic fatty liver disease. Clin Chem Lab Med. 2022;60:243–51.
31. Del Ben M, Overi D, Polimeni L, Carpino G, Labbadia G, Baratta F, et al. Overexpression of the vitronectin V10 subunit in patients with nonalcoholic steatohepatitis: implications for noninvasive diagnosis of NASH. Int J Mol Sci. 2018;19:603.
32. Younossi ZM, Baranova A, Ziegler K, Del Giacco L, Schlauch K, Born TL, et al. A genomic and proteomic study of the spectrum of nonalcoholic fatty liver disease. Hepatology. 2005;42:665–74.
33. Deprince A, Hennuyer N, Kooijman S, Pronk ACM, Baugé E, Lienard V, et al. Apolipoprotein F is reduced in humans with steatosis and controls plasma triglyceride-rich lipoprotein metabolism. Hepatology. 2023;77:1287–302.
34. Wang YB, Zhou BX, Ling YB, Xiong ZY, Li RX, Zhong YS, et al. Decreased expression of ApoF associates with poor prognosis in human hepatocellular carcinoma. Gastroenterol Rep (Oxf). 2019;7:354–60.
35. Sarkar M, VanWagner LB, Terry JG, Carr JJ, Rinella M, Schreiner PJ, et al. Sex hormone-binding globulin levels in young men are associated with nonalcoholic fatty liver disease in midlife. Am J Gastroenterol. 2019;114:758–63.
36. Liu YJ, Kimura M, Li X, Sulc J, Wang Q, Rodríguez-López S, et al. ACMSD inhibition corrects fibrosis, inflammation, and DNA damage in MASLD/MASH. J Hepatol. 2025;82:174–88.
37. Jeong BK, Choi WI, Choi W, Moon J, Lee WH, Choi C, et al. A male mouse model for metabolic dysfunction-associated steatotic liver disease and hepatocellular carcinoma. Nat Commun. 2024;15:6506.
38. Castañé H, Jiménez-Franco A, Hernández-Aguilera A, Martínez-Navidad C, Cambra-Cortés V, Onoiu AI, et al. Multi-omics profiling reveals altered mitochondrial metabolism in adipose tissue from patients with metabolic dysfunction-associated steatohepatitis. EBioMedicine. 2025;111:105532.
39. Oh S, Baek YH, Jung S, Yoon S, Kang B, Han SH, et al. Identification of signature gene set as highly accurate determination of metabolic dysfunction-associated steatotic liver disease progression. Clin Mol Hepatol. 2024;30:247–62.
40. Huang Y, Wang C, Zhou T, Xie F, Liu Z, Xu H, et al. Lumican promotes calcific aortic valve disease through H3 histone lactylation. Eur Heart J. 2024;45:3871–85.
41. Subudhi S, Drescher HK, Dichtel LE, Bartsch LM, Chung RT, Hutter MM, et al. Distinct hepatic gene-expression patterns of NAFLD in patients with obesity. Hepatol Commun. 2022;6:77–89.
42. Baxter RC. Endocrine and cellular physiology and pathology of the insulin-like growth factor acid-labile subunit. Nat Rev Endocrinol. 2024;20:414–25.
43. Lv S, Zhou Y, Chen J, Yuan H, Zhang ZN, Luan B. Hepatic ER stress suppresses adipose browning through ATF4-CIRP-ANGPTL3 cascade. Cell Rep. 2022;40:111422.
44. Khoury M, Guo Q, Furuta K, Correia C, Meroueh C, Kim Lee HS, et al. Glycogen synthase kinase 3 activity enhances liver inflammation in MASH. JHEP Rep. 2024;6:101073.
45. Sabatini S, Sen P, Carli F, Pezzica S, Rosso C, Lembo E, et al. Hepatic glucose production rises with the histological severity of metabolic dysfunction-associated steatohepatitis. Cell Rep Med. 2024;5:101820.

Publisher's Note